Deep-Sea Research I 95 (2015) 54–66

Contents lists available at ScienceDirect

Deep-Sea Research I

journal homepage: www.elsevier.com/locate/dsri

Hydrodynamics over the Gulf of Valencia continental slope and their role in sediment transport

M. Ribó [a,*], P. Puig [a], H. van Haren [b]

[a] Institut de Ciències del Mar, ICM-CSIC, Barcelona, Spain
[b] Royal Netherlands Institute for Sea Research, NIOZ, Texel, The Netherlands

ARTICLE INFO

Article history:
Received 2 June 2014
Received in revised form
8 October 2014
Accepted 13 October 2014
Available online 23 October 2014

Keywords:
Hydrodynamics
Sediment transport
Gulf of Valencia
Continental slope
Western Mediterranean

ABSTRACT

Circulation patterns and sediment dynamics were studied over the Gulf of Valencia (GoV) continental slope during spring and winter 2011–2012. Two moorings were deployed at two locations; at 450 m depth from February to May 2011, and at 572 m depth from October 2011 to February 2012. At both mooring sites, observations were made of currents, temperature and near-bottom turbidity within the lowermost 80 m above the seafloor. The temperature measurements allowed distinction of the different water masses and their temporal evolution. The fluctuations of the boundary between the Western Mediterranean Deep Water (WMDW) and the Levantine Intermediate Water (LIW) masses were monitored, and several intrusions of Western Mediterranean Intermediate Water (WIW) were observed, generally coinciding with changes in current direction. At both mooring sites, the currents generally maintained low velocities $< 10\ cm\ s^{-1}$, with several pulses of magnitude increases $> 20\ cm\ s^{-1}$, and few reaching up to $35\ cm\ s^{-1}$, associated with mesoscale eddies and topographic waves. The current direction was mainly towards the SSE on the first deployment and to the ESE on the second deployment. This second location was affected by a strong bottom offshore veering presumably generated by local topographic effects. Increases in suspended sediment concentrations (SSC) were observed repeatedly throughout the records, reaching values $> 3\ mg\ l^{-1}$. However, these SSC variations were uncorrelated with changes in velocity magnitude and direction and/or with temperature oscillations. Results presented in this paper highlight the complex relation between the hydrodynamics and sediment transport over the GoV continental slope, and suggest that other potential sediment resuspension mechanism not linked with current fluctuations, might play a key role in the present-day sedimentary dynamics. Resuspension due to bottom trawling appears to be the most plausible mechanism.

1. Introduction

Ocean management efforts have focused on the need to identify the actual mechanisms that control the sediment transport and the final fate of most particulate matter introduced from the continental to the marine system. Fine particles (settling and suspended) are responsible for much of the flux of matter and energy in the marine environment, playing a key role in the global oceanic biogeochemical cycles and in the marine ecosystems (Asper et al., 1992). Sedimentary processes control the transport of most particulate elements introduced or generated in the oceans, being especially important in continental margins because of the large material inputs from both fluvial and high productivity coastal waters (Walsh, 1991). However, the study of sedimentary dynamics on continental margins is complex because in these areas coexist anthropogenic activities and oceanographic processes that combine their action to influence sediment particles transport and fate.

The general oceanographic circulation of the northwestern Mediterranean has been widely described in numerous studies (Font, 1987; Millot, 1999; Robinson and Leslie, 2001; Salat et al., 2002; Millot and Taupier-Letage, 2005; López-Jurado et al., 2008), with specific ones devoted to the Balearic Sea (García et al., 1994; Pinot et al., 1994, 1995, 2002; Salat, 1995; Monserrat et al., 2008). The Gulf of Valencia (GoV) is located at the southern part of the Balearic Sea between the Ebro continental margin and the promontory Cap La Nao (Fig. 1). Circulation in the GoV is characterized by water mass mixing between the Northern Current flowing along the continental slope towards the southwest carrying old Atlantic Waters (oAW), and the northward intrusions of recent Atlantic Waters (rAW) through the Ibiza Channel (Pinot et al., 2002). Below these surface waters, three water masses types are also present: from 200 to 400 m depth the seasonal Western Mediterranean Intermediate Water (WIW) is found, characterized by a temperature relative minimum of 12.7 °C and salinity of 38.1. Between 400 and

* Corresponding author.

http://dx.doi.org/10.1016/j.dsr.2014.10.004
0967-0637/

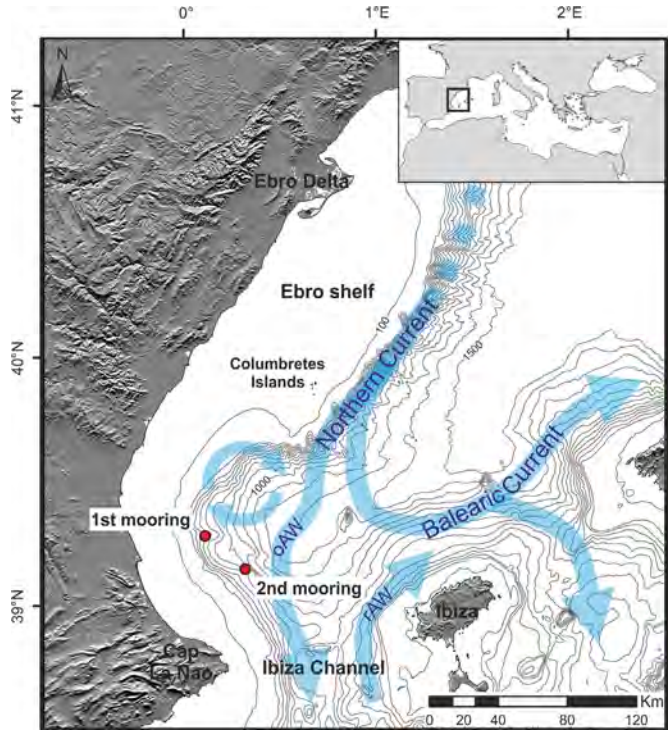

Fig. 1. Bathymetric map of the southern part of the Balearic Sea, including the Gulf of Valencia, showing the major currents characterizing the regional surface circulation scheme (blue arrows, synthesized from Pinot et al (2002) and Ribó et al. (2013)). Red dots indicate the mooring locations. (For interpretation of the references to color in this figure legend, the reader is referred to the web version of this article.)

700 m depth, the Levantine Intermediate Water (LIW) is present, being characterized by temperature and salinity relative maxima of 13.3 °C and 38.5, respectively. Below 700 m depth, the Western Mediterranean Deep Waters (WMDW) is found, with temperature of 13 °C and salinity of 38.4 (Salat and Font, 1987; Font, 1987; Font et al., 1988). The LIW is carried in the lower part of the Northern Current, and bifurcates to the north of the Ibiza Channel as do the surface waters (Font, 1987; Pinot and Ganachaud, 1999; Pinot et al., 2002). The WIW is formed seasonally, and its production is related to the formation of cold and dense waters in the northwestern Mediterranean in winter. When the WIW is present in or nearby the Ibiza Channel, it usually deflects downwards the LIW, which normally occupies shallower levels when the WIW is absent (Monserrat et al., 2008).

Circulation in the GoV has been described as seasonally dominated by the Northern Current entering as an unstable meandering jet (García et al., 1994; Pinot et al., 1995, 2002). The meandering activity is strongest in winter starting in November–December and persisting until May, anticyclonic meanders being the most developed ones, with a characteristic size of typically 20 to 40 km. On several occasions, anticyclonic vortex eddies are found in the interior of the meanders, corresponding to the mature stage of the instability (Pinot et al., 2002). These mesoscale eddies were described to be presumably produced by the instabilities of the regional circulation, caused by the interactions with the bathymetry (Millot, 1999). As winter forcing relaxes in spring–summer, the Northern Current weakens, and the meandering reduces in parallel with the weakening of the current (Pinot et al., 2002).

Previous studies using moored instrumentation on the Ebro shelf (Puig et al., 2001; Palanques et al., 2002) have suggested that the GoV receives most of the sediment transported southwestwards along the Ebro margin. A recent hydrographic study (Ribó et al., 2013), however, has shown a preferential off-shelf sediment export at the southern end of the GoV, where an important detachment of particulate matter was observed off Cap La Nao, extending seawards all across the Ibiza Channel. Ribó et al. (2013) also described the presence of several near-bottom and mid-slope turbid layers, mainly between 400 and 600 m. The occurrence of such nepheloid layers was related to the presence of internal waves on the mid-slope region causing resuspension and/or inhibiting suspended sediment deposition, as it has been described in other areas (Cacchione and Drake, 1986; Puig et al., 2004; Hosegood and van Haren, 2004; Bonnin et al., 2006).

Internal wave motions on the GoV continental slope have been recently monitored and characterized through detailed mooring observations, and consisted on stratified perturbations and convective overturns reaching the bottom (van Haren et al., 2013). Van Haren et al. (2013) observed a ~11-day periodic turbulence, which moved cold WMDW underneath the relatively warmer LIW, simultaneously enlarging the bottom boundary layer as might be induced in a wave motion or a bore. This turbulence appears convective, producing shear-induced Kelvin–Helmholtz overturning instabilities reaching the entire sampled water column (i.e. 60 m) above the bottom. The authors observed that inertial motions superimposed on the large-scale processes provided very large convective turbulence, and described that the varying of turbulence intensity could affect the generation of short internal waves near the local buoyancy frequency. It was suggested that the turbulent processes associated with such near-inertial internal waves might play an important role in the nepheloid layer formation, dispersing and maintaining the suspended particles over the slope.

In this paper, we analyze the current fluctuations and the temperature variations at two locations on the GoV continental slope, and relate these records with variations on near-bottom suspended sediment concentration (SSC). In addition, trawling activity in the study area has been also analyzed since previous studies (e.g. Martín et al. 2014) have evidenced that deep bottom trawling on the NW Mediterranean can replace natural processes as the main driving force of sediment resuspension on continental regions, and generate increases on near-bottom SSC, similar to the ones recorded over the GoV continental slope. The aim of this paper is to improve the understanding on the hydrographic structure and the regional circulation, and discuss the relation with the sedimentary dynamics over the GoV continental slope, assessing the role that mesoscale current variability and the near-inertial internal waves might play in the sediment transport on this region.

2. Methods

During this study, the observational work consisted of time series measurements at two locations over the GoV continental slope using instrumented moorings. The first mooring was deployed from mid-February 2011 to mid-May 2011, located at 39° 16′N and 0° 06′E, at 450 m depth, while the second one was moored from October 2011 to mid-February 2012, at 39° 10′N and 0° 20′E, at 572 m water depth (Fig. 1). Both moorings were deployed on structural highs over the continental slope, chosen using the bathymetric map of the study area and in agreement with the local fishermen, to avoid interfering with bottom trawling activities. The two moorings were equipped with a downward-looking 300 kHz four-beam RDI Acoustic Doppler Current Profiler (ADCP), located at 80 m above bottom (mab), covering 40 cells of 2 m size vertically. They sampled at a rate of once per 10 min. Noise was recorded near the seafloor due to direct vertical sidelobe reflection, and therefore these data were not taken into account. The first cell with reliable data was at 8 mab. Both moorings also included a thermistor string composed of several 'NIOZ4' self-contained temperature sensors sampling at 1 Hz, with a precision of better than 0.001 °C (van Haren et al., 2009).

Unfortunately, during the first mooring deployment, these temperature sensors had battery issues, and consequently very limited data was recorded. Data from the high-frequency temperature sensors installed on the second mooring deployment have been previously described in detail in van Haren et al. (2013). Additionally, in between the thermistor sensors, 10 Optical Backscatter Sensors (OBS) were placed along the mooring, positioned every 5 to 10 m, with the lowest sensor at 5 mab. These OBS measured pressure (resolution < 0.005% full scale), temperature (resolution < 0.003 °C) and turbidity (light source wavelength of 880 nm) with a sampling rate of once per 15 s. For the purpose of this paper, the temperature data from the OBS records collected in both moorings will be analyzed to allow comparisons between both observational sites.

Before each mooring deployment and after each mooring recovery, two conductivity–temperature–depth (CTD) profile casts were performed with a Seabird 911 probe, with the entire thermistor and OBS string coiled and attached to the CTD frame. Temperature and salinity profiles were used to characterize the hydrographic structure of the study site, and to calibrate and correct the measurements of all the temperature sensors mounted on the moorings. After correction, the recorded temperature was converted into potential temperature (θ). The OBS measured turbidity by detecting scattered light from suspended particles in the water in Formazin Turbidity Units (FTU). The sensor gain was set at 100× for a sensitive of 200 mV/FTU and a range of 0–25 FTU, with an error of 2% up to the maximum concentration. The readings were converted to estimates of suspended

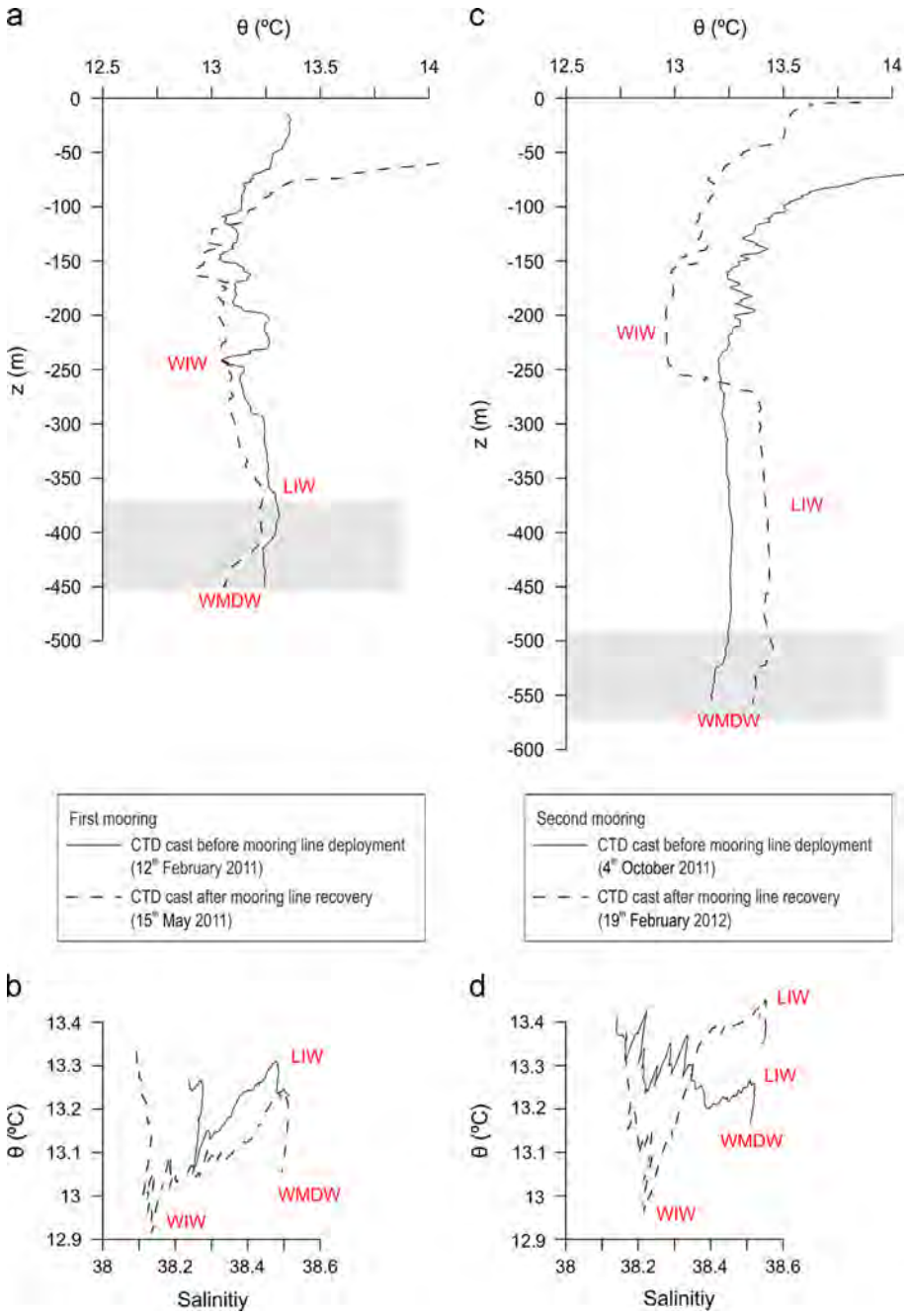

Fig. 2. Potential temperature profiles and T–S diagrams from CTD-data before the mooring deployment (solid line) and after the mooring recovery (dashed line), near the first (a and b) and the second (c and d) mooring locations. LIW: Levantine Intermediate Water; WIW: Western Mediterranean Intermediate Water; WMDW: Western Mediterranean Deep Waters.

sediment concentrations (SSC) following the general equation SSC ($mg\,l^{-1}$) = 1.74*(FTU − FTU_{min}) based on the calibration defined by Guillén et al. (2000). Values were adapted to the measurements made in the study site, where FTU_{min} is the minimum turbidity recorded by the sensor during the two mooring deployment periods. Unfortunately, nearly all OBS were rapidly biofouled and the signal couldn't be used. Only the lowermost OBS placed at 5 mab provided reliable data with no signs of biofouling through the entire deployment.

Current and sediment flux progressive vector diagrams were computed, and near-bottom instantaneous sediment fluxes and time-integrated cumulative sediment transport were also calculated, using the current measurements at 8 mab and the SSC values at 5 mab. To obtain the along- and across-slope instantaneous sediment fluxes and the along- and across-slope cumulative sediment transport, the coordinate system was rotated to the main isobath orientation of each mooring site, using the bathymetric map of the study area as reference (Fig. 1). Current components from the first mooring were rotated 10° anticlockwise and the positive along-slope direction was 170°. The velocity components from the second mooring were rotated 75° anticlockwise and the positive along-slope direction was 105°.

In addition, to assess the potential role that resuspension processes caused by bottom trawling activities could have on the observed SSC records, the Fishing Monitoring Centre of the Spanish Secretariat of Maritime Fishing (SEGEMAR) provided data from the satellite-based tracking Vessel Monitoring Systems (VMS) of fishing trawlers operating in the Gulf of Valencia. The requested VMS data was from February 2011 to February 2012, which includes the two mooring deployment periods, and the information was provided encrypted (i.e. without the ship's identification) and consisted of the vessel's position, heading and speed measurements, recorded approximately every 2 h. VMS data was also provided filtered, up to maximum speeds of 5 kt, allowing identification of the positions of the vessels during trawling activities and not while steaming (speeds > 5 kt) towards the port or the fishing grounds.

3. Results

3.1. Hydrographic structure

Potential temperature vertical profiles and θ-S diagrams are displayed in Fig. 2. The signatures of WIW, LIW and WMDW were recognized by identifying the temperature and salinity values characteristic of each water mass (see Section 1), and also the variation of the water masses position over the GoV continental slope was evidenced. Although the first mooring was located at 450 m depth, and the second at 572 m depth, both measured up to 80 mab (grey band in Fig. 2) where the LIW and WMDW water mass interface was located. On the first mooring site, before the deployment, the signature of WIW and LIW detected in the CTD cast was not evident (Fig. 2a and b solid lines). However, after the first mooring recovery, the WIW, LIW and WMDW signatures were clearer (Fig. 2b dashed line), and a decrease of temperature was recorded below 100 m (Fig. 2a and b). At the second mooring site, no presence of WIW was observed before the deployment, and the temperature profile was very uniform with a slight decrease where the WMDW was located, caused by the weak presence of LIW (Fig. 2c and d solid line). In contrast, after the mooring recovery, strong WIW and LIW signatures were recorded on the vertical profile (Fig. 2c dashed line), being clearly identified on the θ-S diagram (Fig. 2d dashed line).

3.2. Hydrodynamics over the Gulf of Valencia continental slope

3.2.1. Winter–spring 2011

The first mooring was deployed in the central part of the Gulf of Valencia (GoV) at 450 m depth (Fig. 1) from mid-February to mid-May 2011. During the first 20 days of the deployment, until the 3rd March 2011, variations of current magnitude (Fig. 3a) and direction (Fig. 3b) were dominated by near-inertial motions. The inertial motions, defined by the Coriolis parameter (f) which depends on the rotation rate of the Earth ($\Omega = 7.292 \times 10^{-5}$ s) and the latitude

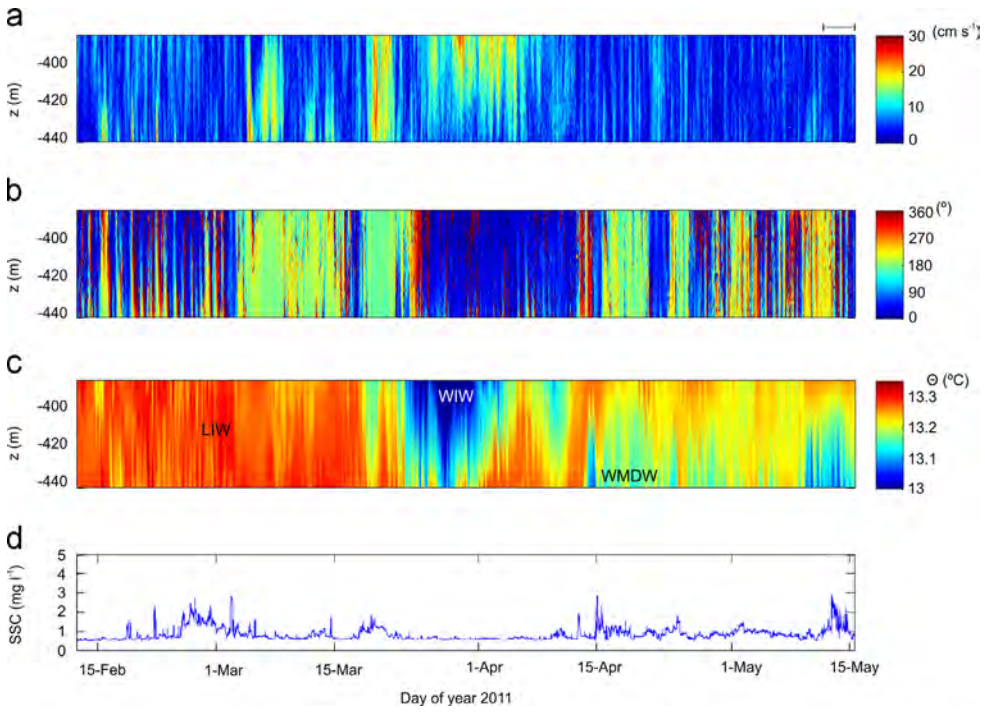

Fig. 3. (a) Current magnitude (cm s^{-1}), (b) current direction (°) from ADCP, and (c) potential temperature and (d) near-bottom turbidity records from the OBS, from the first mooring LIW: Levantine Intermediate Water; WIW: Western Mediterranean Intermediate Water; WMDW: Western Mediterranean Deep Waters.

(φ), were calculated at the study site (φ=39° N) following the equation $f=2\,\Omega\,\sin\,\varphi$, and have a periodicity of 18.8 h. They are generated via geostrophic adjustment following the passage of disturbances by fronts, mainly atmospheric ones. After an atmospheric disturbance passage, they propagate downward as inertial waves are the only inertio-gravity waves that can pass through both homogeneous and stratified layers (e.g., van Haren and Millot, 2005).

During the first 20 days of the mooring deployment, current magnitudes maintained relatively low values <10 cm s^{-1}, with some noticeable near-bottom increases, up to 25 cm s^{-1} (Fig. 3a). During this period, current direction at the upper levels was almost perpendicular to the direction of currents near the seafloor, which was mainly towards the south-southeast (Fig. 3b). The LIW water mass occupied the entire sampled water during this first period, showing θ values of ~13.25 °C and displaying several temperature oscillations of 0.05 °C (Fig. 3c). Near-bottom turbidity at the beginning of the record presented values of 0.5 mg l^{-1} (Fig. 3d), alternating with sharp peaks of >1 mg l^{-1} followed by an increase of up to 2.9 mg l^{-1} starting the 25th of February 2011 and lasting for a week, without a clear relation with changes in the current magnitude and direction and/or temperature oscillations. On the 3rd of March, an abrupt change of current direction towards the south was recorded (Fig. 3b), correlated with several increases of the near-bottom velocity, reaching values up to 35 cm s^{-1}(the 5th of March) (Fig. 3a), and a slight decrease in temperature, mainly at the upper levels (Fig. 3c). These conditions lasted for 13 days, until the 16th of March, when a rapid change in current direction towards the north was recorded during three days (Fig. 3b). Immediately afterward, on the 19th of March, current direction rapidly changed again towards the south coinciding with an abrupt increase in velocity magnitude throughout the entire sampled water column that only lasted for one day, followed by a colder water intrusion (Fig. 3c), and a slight increase of near-bottom SSC (Fig. 3d).

On the 22nd of March, increases of current velocities >20 cm s^{-1} were observed at the upper levels only, between 380 and 420 m, and not near the bottom (Fig. 3a). Current direction abruptly changed towards the north (Fig. 3b), accompanied by a strong cooling of the water temperature, reaching values of <13.1 °C, caused by the intrusion of WIW (Fig. 3c). The arrival of this cold water mass was concurrent with minimum values of near-bottom turbidity (Fig. 3d). On the 5th of April, temperature progressively started to increase again (Fig. 3c), coinciding with a decrease of the current magnitude at shallow levels (Fig. 3a), whilst the current direction was maintained northward until the 15th of April (Fig. 3b). This temperature increase corresponded to the return of the LIW in the sampled range, which rapidly moved upwards (and presumably seaward) allowing the entrance of WMDW in the lowermost part of the range, decreasing the near-bottom temperatures below 13.1 °C (Fig. 3c).

From the 15th of April to the end of the record, measured temperatures corresponded to the interface of the LIW and WMDW water masses, at depths between 400 and 420 m, presenting continuous oscillations between 13.15 and 13.25 °C reaching all the way to the bottom (Fig. 3c). Current direction presented several shifts, changing sharply from the north to the south with a periodicity of ~5 days, superimposed over low-frequency oscillations (Fig. 3b). In addition, current magnitude was relatively low, between 5 and 10 cm s^{-1} (Fig. 3a), and SSC varied between 0.6 and 1.6 mg l^{-1}, with an increase at the end of the time series reaching values up to 3 mg l^{-1} (Fig. 3d).

3.2.2. Winter 2011–2012

During the 2nd deployment, the current magnitudes maintained relatively low values <10 cm s^{-1}, alternating with periods of near-bottom velocity increases occurring with 5 and 20 day periodicity (Fig. 4a). Current direction was mainly in an ESE direction (Fig. 4b), although reversals in the current direction towards the north were observed repeatedly, coinciding with periods of low current velocities, dominated by near-inertial motions (see Van Haren et al. (2013) for details). Since the mooring was located across the interface between the LIW and the WMDW, temperature registered fluctuations from 13.15 to 13.25 °C (Fig. 4c), with intrusions of colder waters near the bottom coincident with periods of increased near-bottom current velocities. However, from the second half of the time series, the temperature progressively increased, reaching maximum values of 13.4 °C (over the color scale in Fig. 4c), due to the downslope displacement of the

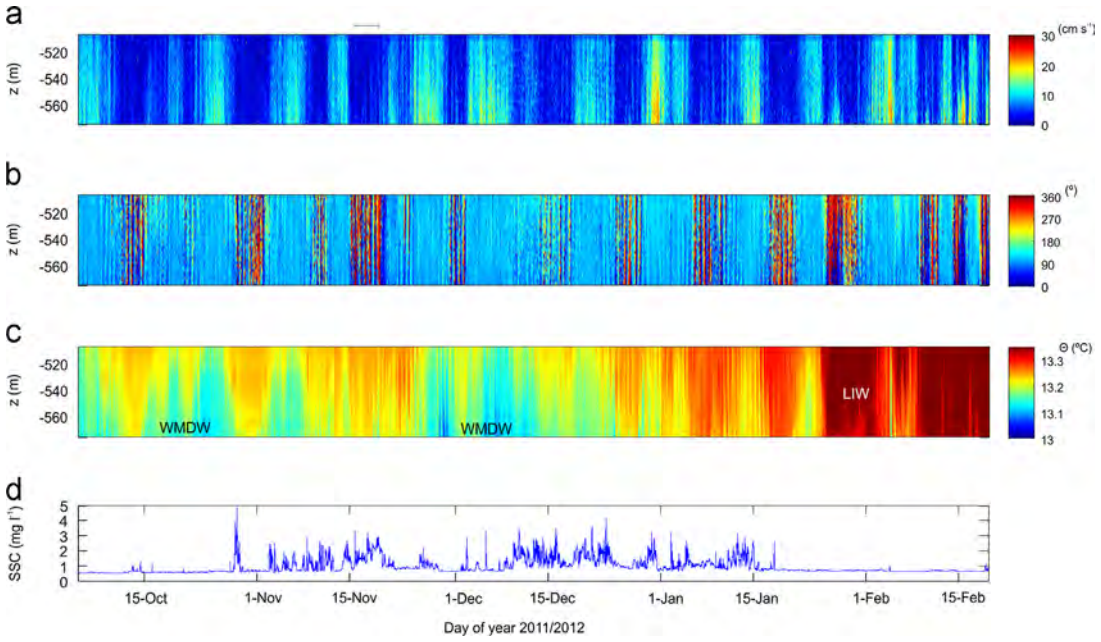

Fig. 4. As Fig. 3, but for the second mooring.

LIW water mass, presumably caused by the intrusion of the WIW at upper levels (Fig. 2c). This warming trend was only disrupted by the intrusion of some cold water pulses that were recorded near the bottom from the 4th to the 9th of February 2012 (Fig. 4c).

The near-bottom turbidity maintained minimum values $\sim$0.5 mg l^{-1} during the first 20 days, with small isolated peaks of $\sim$1 mg l^{-1}, until a sharp increase up to 5 mg l^{-1} was registered on the 28th of October 2011 (Fig. 4d). This event lasted for several hours. From the 3rd of November 2011 to the 18th of January 2012, the SSC increased again repeatedly, alternating between periods with values oscillating between 2.5 and 3.5 mg l^{-1} and others with minimum background values (Fig. 4d). Such increases in SSC showed no relation with the current magnitude and direction variations. From the 18th of January 2012 until the end of the record, SSC showed again minimum values of $\sim$0.5 mg l^{-1}. It is to be noted that on the 31st of December 2011 a near-bottom current velocity increase up to 28 cm s^{-1} was registered (Fig. 4a), coincident with an increase of near-bottom turbidity, up to 3 mg l^{-1}. However, a similar event occurred on the 4th of February 2012, reaching up to 21 cm s^{-1} did not generate any increase of SSC (Fig. 4d).

3.3. *Progressive vectors of currents and near-bottom sediment transport*

As it has been shown, currents on the GoV continental slope are highly variable and extremely conditioned by the local bathymetry. Progressive vectors of currents measured each 10 m above the seabed, and progressive vectors of near-bottom horizontal particle fluxes were here analyzed to determine the sediment transport dispersal pathways (Figs. 5 and 6).

Temporal progression of the current vectors at the first mooring site showed strong changes throughout the study period and between different heights (Fig. 5a). Starting on the 12th of February 2011 and for the first 20 days, currents at upper levels (from 30 to 70 mab) were flowing mainly in a northeastern direction (Fig. 5a). Conversely, currents close to the bottom (from 10 to 20 mab) were predominantly directed towards the south and several wiggles were observed, corresponding to current oscillations dominated by near-inertial motions (Fig. 5a). On the 3rd of March a rapid turn in the current direction affected all depths, and currents flowed towards the south-southeast homogeneously through the entire sampled water column until the 22nd of March 2011. During this first period, the progressive near-bottom sediment flux diagram followed the same pattern described by the near-bottom currents, flowing southwards and also being affected by the current direction oscillations (Fig. 5b). On the 22nd of March the currents and near-bottom sediment flux were directed towards the northeast, until mid-April, when both turned again towards the south (Fig. 5a and b). From the 15th of April 2011 to the end of the mooring deployment, current direction was in general towards the south-southeast, showing several reversals (Fig. 5a) that corresponded to the current direction fluctuations, occurring approximately with a 5 day periodicity (Fig. 3b). These changes in the flow direction were more visible on the progressive vector diagram of near-bottom sediment flux (Fig. 5b).

At the second mooring site, in comparison, the progressive vectors at different heights, from 10 to 70 mab, indicated that currents were more consistent through the entire water column (Fig. 6a). Starting the 4th of October of 2011 and throughout the whole record, currents were mainly flowing towards the southeast, following the regional bathymetry, although turning towards the east with depth. Such a behavior indicates that the currents on this mooring site were affected by a strong offshore veering (Fig. 6a), presumably induced by the local topography of the structural high where the mooring was deployed.

During the entire record, several steps were observed in the progressive vectors, coincident with changes in current direction mainly towards the north (Fig. 6a). These periods were characterized by weak current velocities < 10 cm s^{-1} with fluctuating current directions at near-inertial frequencies (Fig. 4a and b). Progressive vectors of near-bottom sediment flux agreed with the current at 10 mab, also reproducing the same changes in the preferable direction of sediment transport (Fig. 6b). At the end of the time series, during the last 20 days, these direction shifts in the current and near-bottom sediment flux progressive vectors were more frequent, continuously turning from the southeast to the

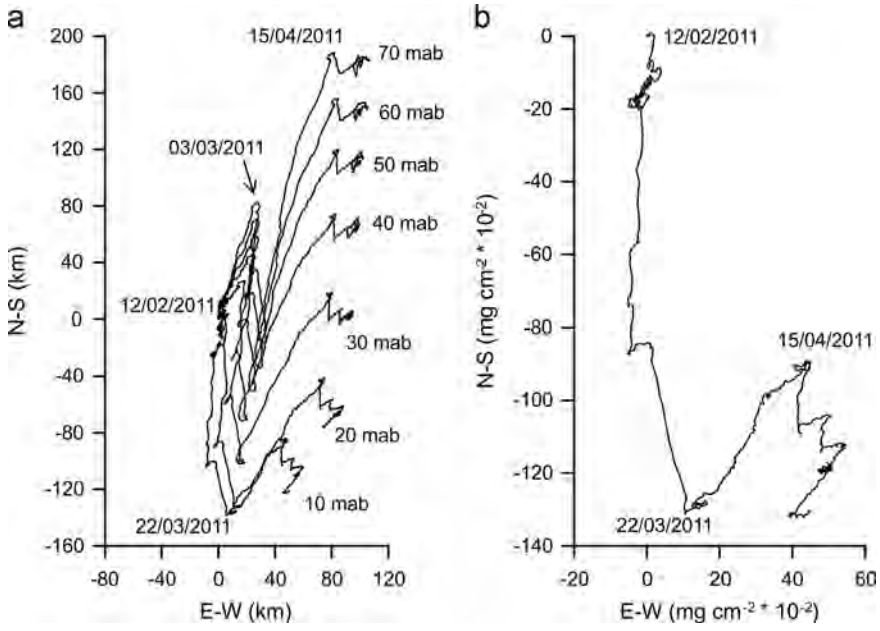

Fig. 5. Progressive vector diagrams computed from (a) current measurements at different depths (indicated in meters above bottom) and (b) near-bottom sediment fluxes at the first mooring.

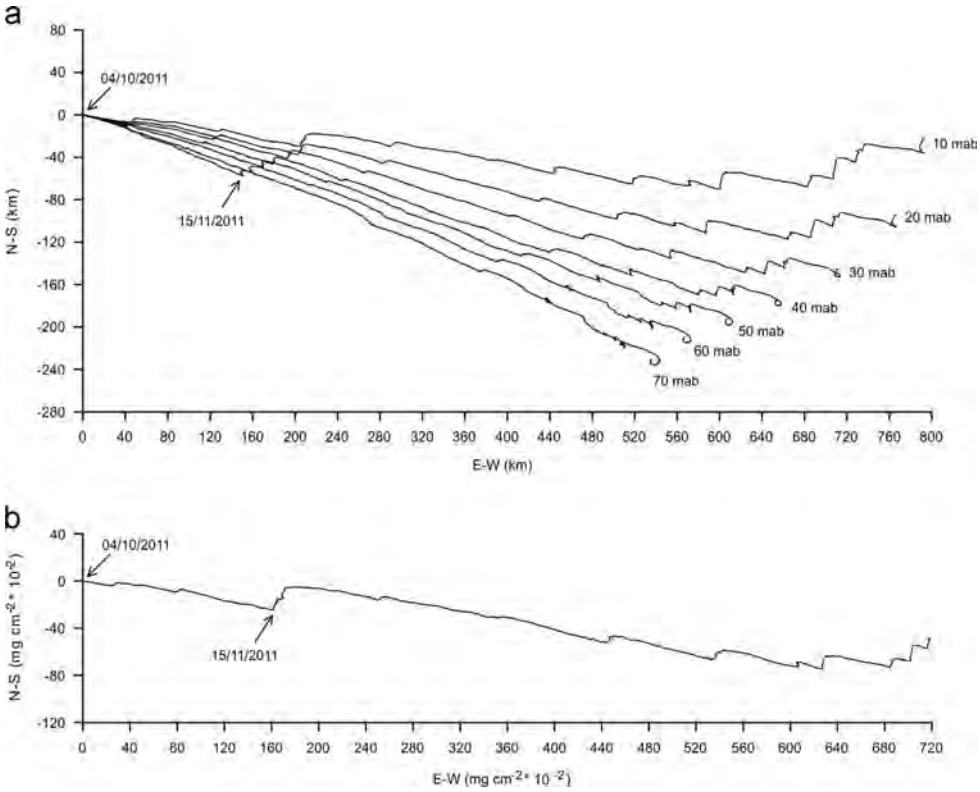

Fig. 6. As Fig. 5, but for the second mooring.

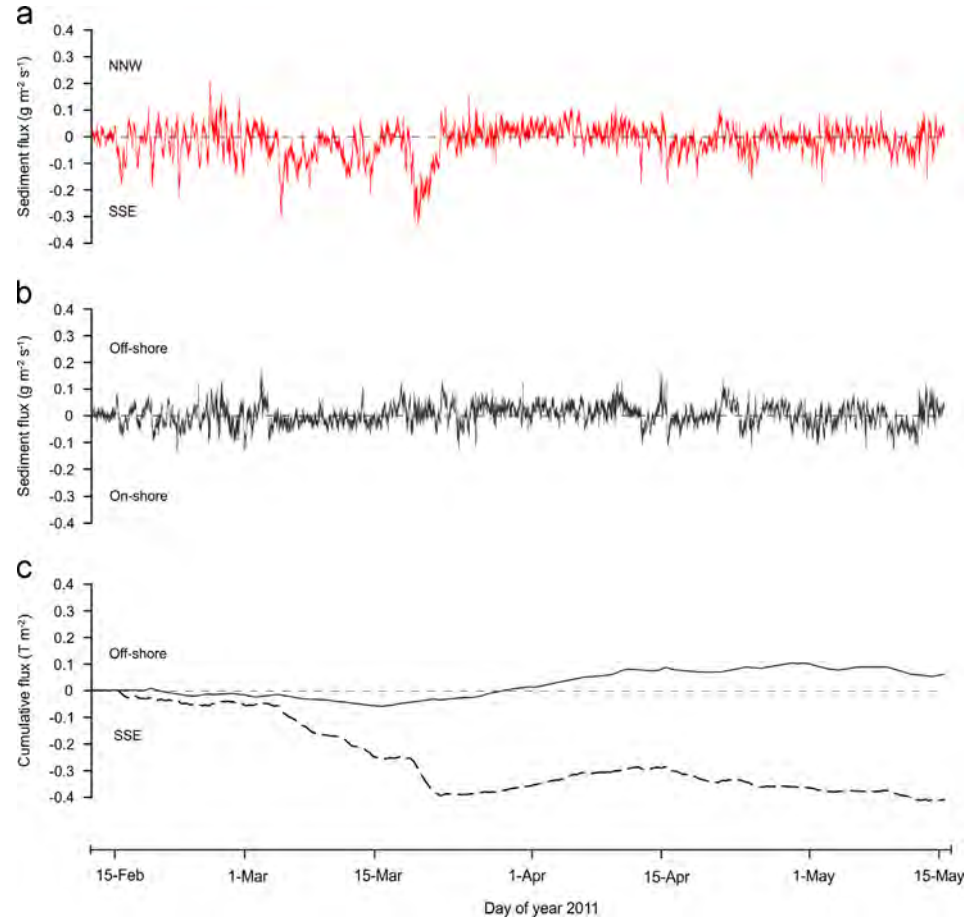

Fig. 7. (a) Instantaneous along-slope suspended sediment flux, (b) instantaneous across-slope suspended sediment flux, and (c) cumulative sediment transport along-slope (dashed line) and across-slope (solid line), at the first mooring site (see location in Fig. 1).

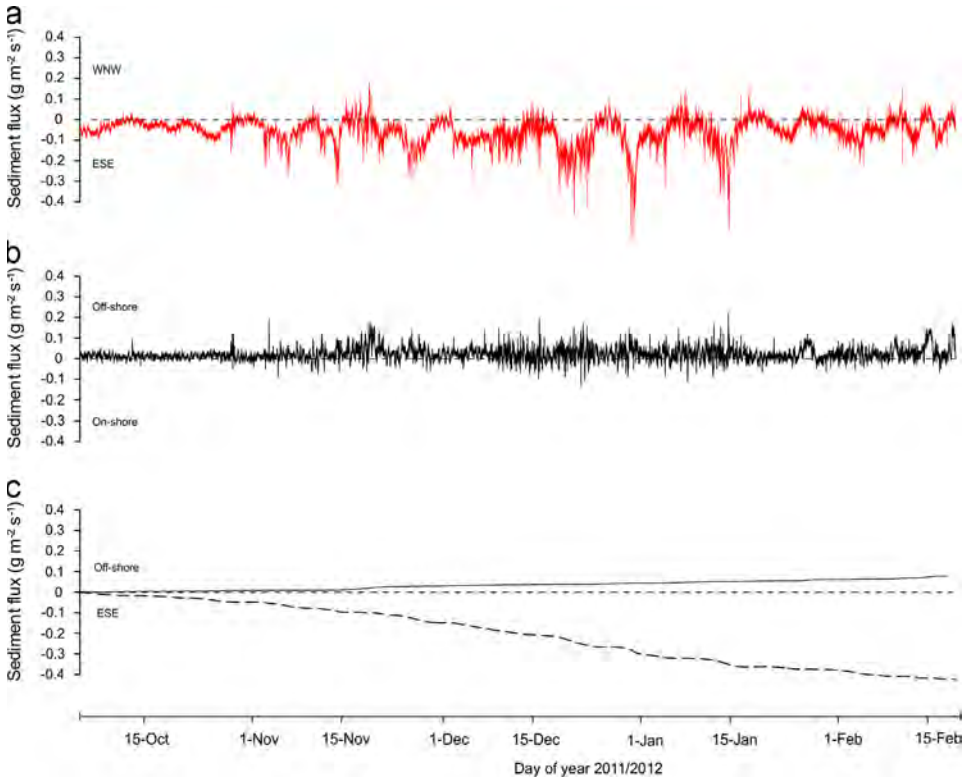

Fig. 8. As Fig. 7, but for the second mooring.

north and southeast again. The changes in direction were stronger closer to the seafloor than higher up in the water column (Fig. 6a), and therefore, they favored near-bottom across-slope sediment transport, being predominantly in the offshore direction (Fig. 6b).

3.4. Along- and across-slope near-bottom sediment fluxes

Instantaneous near-bottom suspended sediment fluxes, and cumulative sediment transport along and across the continental slope, were computed to determine their magnitude and dominant direction (Figs. 7 and 8).

During the first mooring deployment instantaneous along-slope near-bottom suspended sediment flux ranged between 0.21 and 0.33 g m^{-2} s^{-1}, in a NNW and SSE directions respectively (Fig. 7a). Throughout the record, instantaneous sediment fluxes presented oscillations, which seem to be dominated by near-inertial motions since their periodicity is of ~18.8 h. Such fluctuations were also observed in the instantaneous across-slope sediment flux records, with values ranging between 0.17 and 0.13 g m^{-2} s^{-1}, off-shore and on-shore, respectively (Fig. 7b). At the beginning of the mooring deployment, the cumulative sediment transport across- and along-slope was on-shore and in a SSE direction, respectively. From the 3rd of March 2011 there was an increase of the along-slope sediment flux in a SSE direction (Fig. 7a), also reflected on the cumulative sediment transport (Fig. 7c). On the 19th of March 2011, an abrupt increase on the sediment flux towards the SSE was observed (Fig. 7a), but rapidly turning again northwards, until the 22nd of March, coinciding with the intrusion of the WIW (Fig. 3c). From that moment on, the sediment flux was towards the NNW and off-shore (Figs. 7a and b). This trend lasted until the 15th of April 2011, where the along-slope sediment flux slightly turned again towards the SSE, whereas the across-slope component persist off-shore (Fig. 7c). The net across-slope near-bottom sediment transport reached values of ~0.1 T m^{-2} off-shore, while the net along-slope sediment transport was four times higher, ~0.4 T m^{-2} in a SSE direction (Fig. 7c).

On the southern part of the GoV continental slope, where the second mooring was located (Fig. 1), instantaneous along-slope suspended sediment flux continuously oscillated at low frequencies (Fig. 8a), occurring with a 5–20 day periodicity (Fig. 8b). Along-slope instantaneous sediment flux ranged in between 0.16 and 0.61 g m^{-2} s^{-1}, in a WNW and ESE directions, respectively (Fig. 8a). Across-slope instantaneous sediment flux component was less important, with values ranging between 0.23 g m^{-2} s^{-1} off-shore and 0.14 g m^{-2} s^{-1} on-shore (Fig. 8b). During the entire deployment the near-bottom cumulative sediment transport was predominantly in an ESE direction, mainly following the bathymetry, with an important off-shore component (Fig. 8c). The along-slope cumulative transport reached 2.1 T m^{-2}, while the net across-slope component was 0.8 T m^{-2} (Fig. 8c).

4. Discussion

4.1. Role of the water masses and mesoscale current variability

The northwestern Mediterranean regional circulation and the respective role of the different water masses found over the GoV continental slope have been largely described (Font, 1987; Salat, 1995; Millot, 1999). Specifically, the circulation in the GoV region is characterized by a complex variability caused by large instabilities of the Northern Current and by the development of mesoscale eddies, which appear to be strongly influenced by the intrusion of seasonal Western Mediterranean Intermediate Waters (WIW) during winter (Pinot and Ganachaud, 1999; Pinot et al., 2002; López-Jurado et al., 2008; Monserrat et al., 2008). Pinot et al. (2002) observed that post-winter stratification, which is strongly dependent on the amount and properties of the WIW layer, is the main factor controlling the size of the mesoscale eddies. They also observed that these eddies can be slowly funneled through the

Ibiza Channel, causing a complete retroflection of the Northern Current, or they can be trapped inside the GoV for several weeks. Under this second situation, their presence distorts the Northern Current flow without fully obstructing the water exchange through the channel (Millot, 1999; Pinot et al., 2002; López-Jurado et al., 2008).

In the study here presented, the recorded data showed an intrusion of the WIW in early spring 2011 over the central part of the GoV, at 450 m depth (Fig. 3), which deflected the Levantine Intermediate Waters (LIW) downwards, evidenced by an abrupt decrease of the sampled temperature range (Fig. 3c). This cold water intrusion was concurrent with an abrupt change of the current direction towards the north (Fig. 3b) and an increase of the velocity magnitude at the upper levels of the sampled range (Fig. 3a). These observations support the fact that the presence of the WIW water mass in this region can enhance the development of mesoscale structures, affecting the near-bottom circulation over the continental slope. In particular, this current reversal that lasted for 24 days was presumably related to the formation of a mesoscale (typically anticyclonic) eddy that develops over the central part of the GoV continental slope (see mooring position relative to circulation scheme in Fig. 1). These results are also consistent with previous studies conducted over the GoV, which showed that deep channel-size eddies can become trapped for long periods of time north of the Ibiza Channel, particularly during spring (Pinot et al., 2002).

In the southern part of the GoV continental slope, although the incursion of the WIW during spring 2012 was not directly observed, it could be inferred by a downslope displacement of the LIW, and by a progressive increase of the temperature in the sampled range (Fig. 4c). There, the intrusion of the WIW at the upper levels did not cause any major changes in the current direction, probably because an eddy was not formed that year, or because it remained isolated in the central part of the GoV, without affecting the southern part of the continental slope region where the second mooring was located (see mooring position and circulation scheme in Fig. 1).

The presence of the mesoscale variability on this southern region seems to be mainly attributed to the unstable behavior of the Northern Current, which is intensified when entering to the GoV as a meandering jet (Pinot et al., 2002). As has been mentioned, this meandering activity is strongest during winter and can persist until early-spring, and can extend down to the bottom. Such instabilities in the Northern Current could be responsible for the near-bottom fluctuations observed on the southern GoV continental slope, particularly during winter 2011–2012 (Fig. 4). Mooring records during winter-spring 2011 did not show clear evidence of these fluctuations (Fig. 3), presumably because the observations were made in the inner part of the GoV continental slope, sheltered from the general current oscillations. However, the current and sediment flux progressive vectors at this mooring site showed several 5-day oscillations at the end of the record, which are likely to correspond to instabilities of the Northern Current (Fig. 5). Similar low frequency fluctuations have also been described northwards on the northwestern Mediterranean, as in the Ligurian Sea or in the Gulf of Lions, and were identified as topographic waves (Crépon et al., 1982; Sammari et al., 1995; van Haren and Gostiaux, 2011). In the Ligurian Sea, fluctuations of the meandering current were observed parallel to the coastline, with periods of 10–20 days, and perpendicular to the coast with periods of 3–6 days (Sammari et al., 1995). Overall, the current fluctuations observed on the GoV continental slope had a periodicity of 5 to 20 days, and were presumably generated by the topographic waves affecting the study area. Variations in the temperature records also followed such current fluctuations near the bottom, providing evidence of the oscillation of the Western Mediterranean Deep Waters (WMDW) and Levantine Intermediate Waters (LIW) water masses interface close to the seafloor.

As could be clearly observed during the second deployment in the southern GoV continental slope, during periods characterized by low (< 10 cm s^{-1}) current velocities (Fig. 4a) and by changes in current direction at near-inertial frequencies (Fig. 4b), warmer temperatures at the base of the LIW occupy the sampled water column. During periods when near-bottom current magnitudes were high and preferentially oriented towards the SSE (Fig. 4a), colder temperatures from the WMDW affected the lowermost part of the sampled water column. Under these later conditions, fluctuations in the along-slope instantaneous sediment fluxes were recorded (Fig. 8), despite the variations in the SSC-values observed in the records (Fig. 4d), due to higher current velocities and the sustained direction along-margin. This clearly indicates that the sediment transport on the GoV continental slope is mainly controlled by the current fluctuations associated with such topographic waves, even though few, if any, sediment resuspension events could be clearly related with current speed increases.

4.2. *Suspended particles maintained by internal waves*

Detailed observations of the time series showed that overlying the above described current fluctuations associated with the topographic waves, near-inertial motions were recorded, which at the GoV have a periodicity of 18.8 h. The spectra of kinetic energy based on the ADCP data deployed on both moorings are shown in Fig. 9, in which the main current fluctuation periodicities on the study site were determined. It can be observed that the two spectra deviate, presenting the maximum differences, approximately in between 0.1 and 6 cycles per day (cpd). This includes the near-inertial and tidal bands (Fig. 9). The spectrum at the first mooring (black line) is more elevated in this range, with an additional peak at the diurnal frequency and slightly elevated inertial and semidiurnal tidal peaks (Fig. 9). The broad range of elevated variance is attributable to more strongly variable boundary currents, steered by the sloping topography (van Haren and Millot, 2005).

Expansions of 4-days record over the first and second mooring deployments are shown in Figs. 10 and 11, respectively. The near-inertial motions can be observed with the repeated along- and across-slope current increases (panels a, b in Figs. 10 and 11). During both mooring deployments, vertical currents were one order of magnitude smaller than the along- and across-slope currents (Figs. 10 and 11c). During the second mooring deployment, vertical upward currents were more bottom intensified,

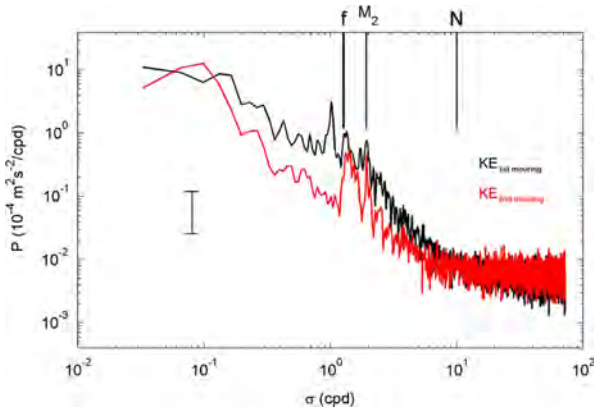

Fig. 9. Spectra of kinetic energy based on the ADCP data of the first (black line) and second (red line) mooring deployments. f indicates the local inertial period (~18.8 h), M_2 the semidiurnal tide (~12.4 h) and N indicates the buoyancy frequency computed from the CTD-data. (For interpretation of the references to color in this figure legend, the reader is referred to the web version of this article.)

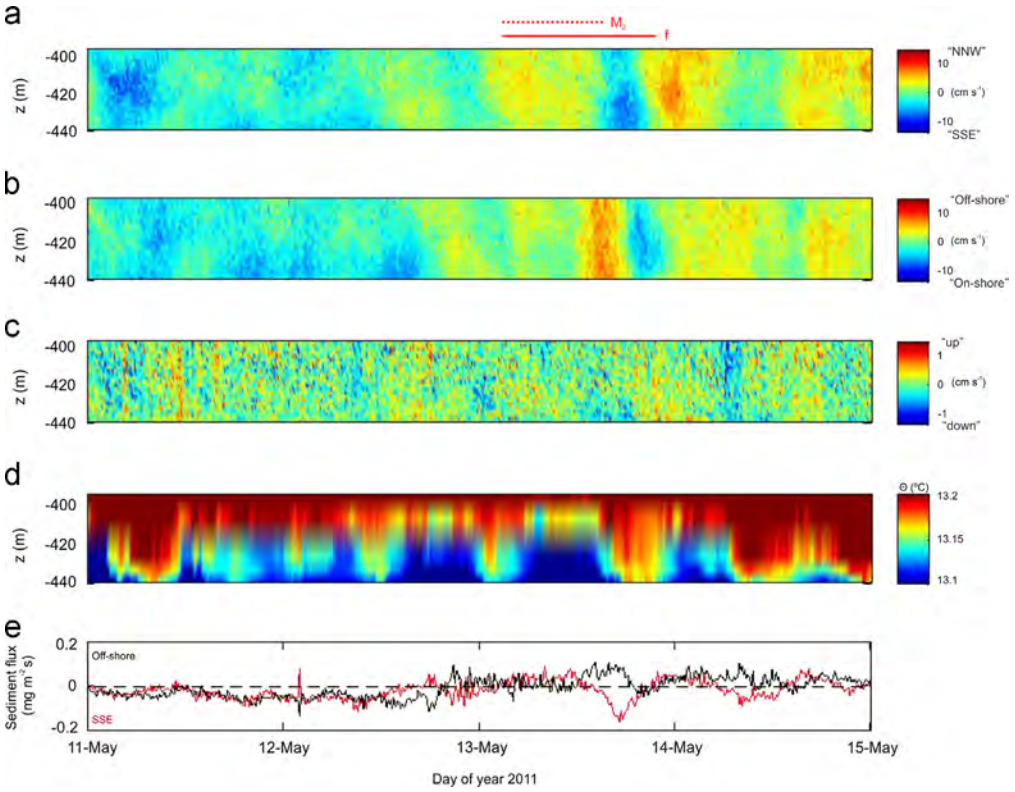

Fig. 10. Four days zoom of the first mooring time series, including detailed observations of (a) along-slope, (b) across-slope, (c) vertical current velocity components (d) temperature and (e) along—(red line) and across—(black line) slope sediment fluxes. Horizontal red bars indicate (solid) the local inertial period ($f \sim 18.8$ h) and (dashed) the semidiurnal lunar tidal periods ($M_2 \sim 12.4$ h). (For interpretation of the references to color in this figure legend, the reader is referred to the web version of this article.)

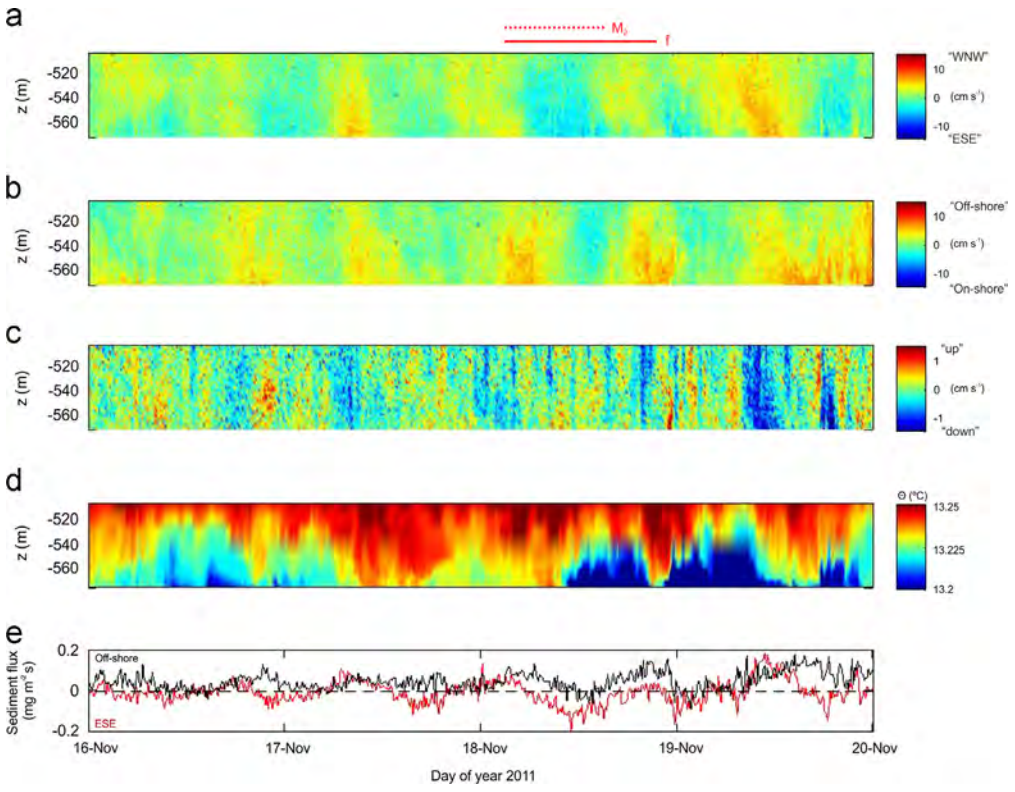

Fig. 11. As Fig. 10, but for the second mooring.

associated with eastern and on-shore currents, following the near-inertial periodicity, and, for the vertical current, shorter periodicities 'high-frequency internal waves' associated with the stratification (Fig. 11c). The above described oscillations caused vertical displacements of the isotherms over 30–60 m, throughout the range of the sampled water column (Figs. 10 and 11d) and similar to previous findings elsewhere (e.g., van Haren and Gostiaux, 2011). These near-inertial temperature variations were mainly

correlated with along and across-slope current oscillations that modulate the sediment flux direction (Figs. 10 and 11e).

Van Haren et al. (2013) associated those temperature variations with internal waves that can generate very large convective turbulence episodes, with large (>50 m) overturns, over the GoV continental slope. These turbulent processes might play an important role in formation and maintenance of bottom nepheloid layers, and in the dispersion of suspended particles towards the ocean interior as intermediate nepheloid layers. Following this approach, Ribó et al. (2013) attributed that the existence of bottom and intermediate nepheloid layers over the GoV continental slope as being generated by the presence of internal waves at the interface between the Levantine Intermediate Waters (LIW) and the Western Mediterranean Deep Water (WMDW). The sediment particles detached from the slope would then be maintained in suspension by the density gradient existing throughout the water column. Several other studies have related the presence of nepheloid layers with internal waves in many different areas (Cacchione and Drake, 1986; Puig et al., 2001, 2004; McPhee-Shaw and Kunze, 2002; McPhee-Shaw, 2006).

It has been also postulated that internal wave turbulence interacting with the bottom of continental slopes can induce sediment resuspension (e.g., Hosegood and van Haren, 2004). However, in the near-bottom turbidity records presented in this study, no resuspension peaks (i.e., sharp increases of SSC) were observed linked to the near-inertial internal waves monitored at the study site. Nevertheless, as it has been previously indicated, they modulate the along- as well as the across-slope sediment flux oscillations, and follow the current direction fluctuations at the same near-inertial time scale (Figs. 10 and 11e). This indicates that the across-slope sediment transport in the GoV margin is mainly controlled by such near-inertial motions, which, over time, preferentially advect suspended particles off-shore (see Fig. 6b). Thus, these results reveal that internal waves interacting with the GoV continental slope play an important role in the maintenance of the suspended sediment that is being advected along- and across-slope, although no sediment resuspension process seems to be associated to them.

4.3. Role of bottom trawling

As has been emphasized, the unexpected high SSC peaks observed at both mooring sites could not be related with any of the hydrodynamics processes operating on the GoV continental slope. This suggests that other potential resuspension mechanisms unrelated with current fluctuations might play an important role in causing the observed sharp and short-lived SSC increases that have been observed in this study and that contribute to the present-day sedimentary dynamics.

Surprisingly, unusual high values of near-bottom turbidity of 3–5 mg l^{-1} were recorded near the bottom during specific periods during both mooring deployments (i.e. 15th of April 2011 in Fig. 3d and from 28th to 30th of October 2011 in Fig. 4d). Such values appear to be much higher than the SSC values recorded by means of hydrographic profiles conducted within the well-developed bottom nepheloid layers observed on the GoV continental slope, which were $\sim$0.6 mg l^{-1} (Ribó et al., 2013). Additionally, at the beginning of the record of the second mooring site (Fig. 4d), near-bottom turbidity maintained background values of $\sim$0.5 mg l^{-1}, lasting for almost the first month, that agreed with the SSC obtained during the hydrographic surveys, but suddenly the SSC increased. Several peaks (up to $\sim$3 mg l^{-1}) were recorded during almost the next two months, in the middle of the monitoring period. Background values were again recorded over one month, until the end of the mooring deployment (Fig. 4d). This anomalous progress of the near-bottom turbidity during winter 2011–2012, with no correlation with changes in current direction and/or magnitude, indicate, a possible external factor controlling the SSC increases on the GoV continental slope during certain periods. Also, no correlations were found during the period with anomalous high SSC and the occurrence of major storms in the study area or flood events from the Ebro or other nearby rivers (data not shown).

Several studies have demonstrated that resuspension by bottom trawling activities can create turbid clouds of high suspended sediments concentration, which have been observed mainly on continental shelves (Churchill, 1989; Schoellhamer, 1996; Stavrakakis et al., 2000; Palanques et al., 2001; Durrieu de Madron et al., 2005; Ferré

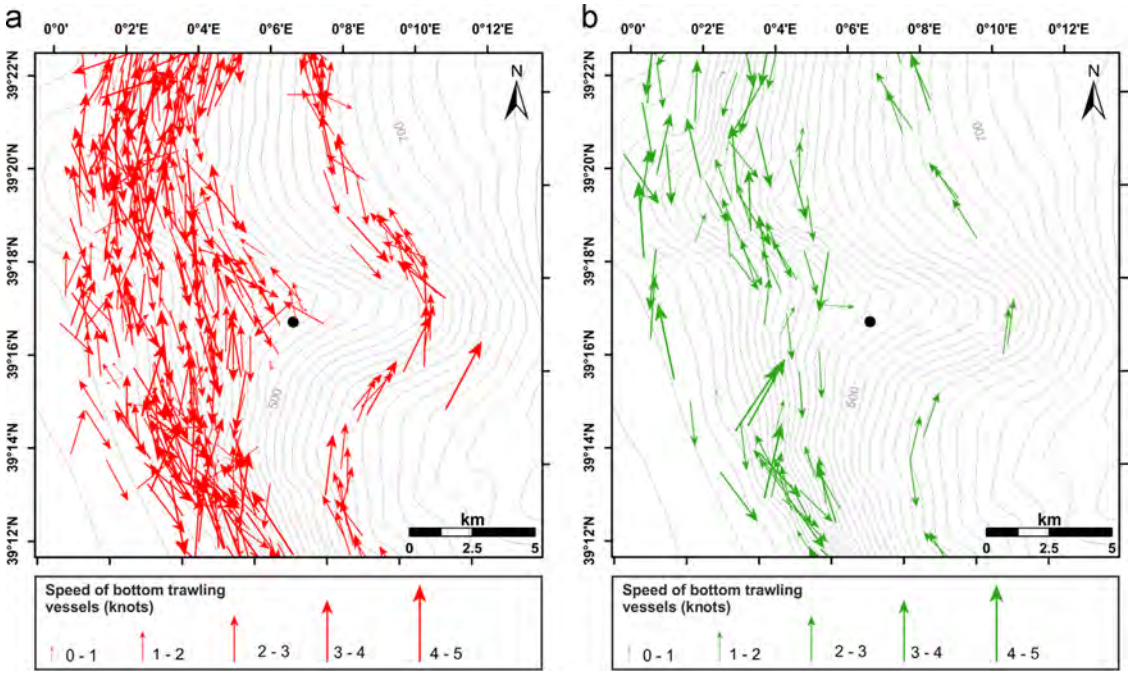

Fig. 12. Position, heading and speed VMS data of bottom trawling vessels fishing nearby the first mooring location (black dot), (a) during high SSC values from the 18th of February to the 22nd of March 2011, and from the 11th April to the 13th of May 2011, and (b) during low/background values from the 24th of March to the 8th of April 2011.

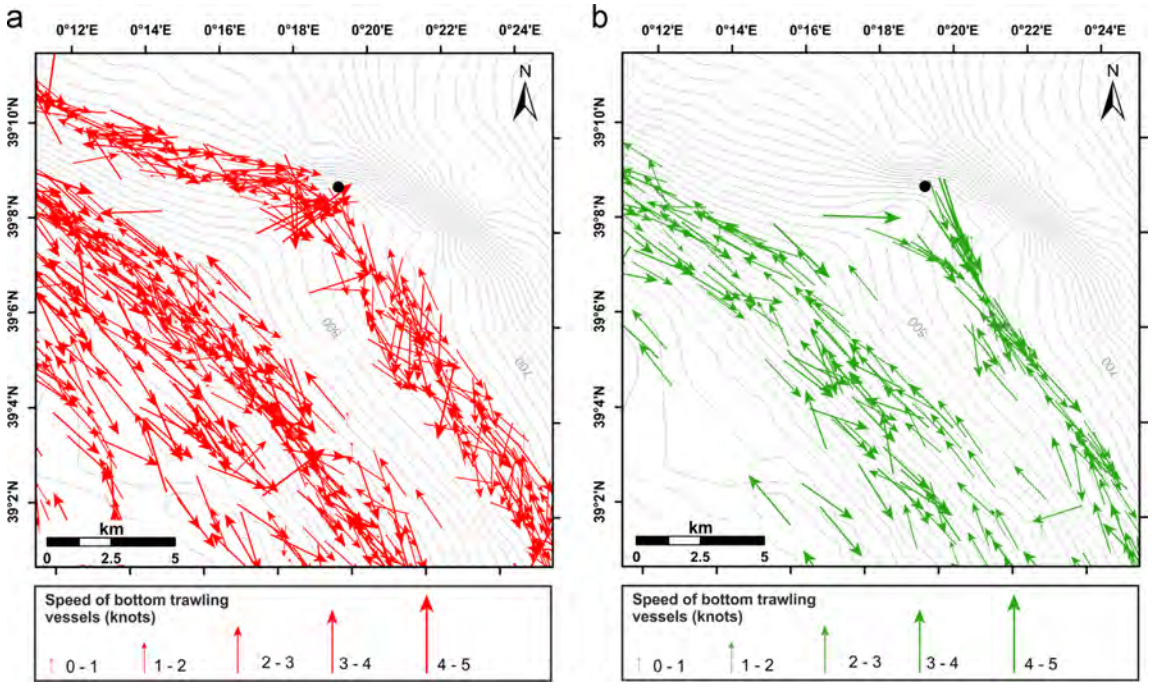

Fig. 13. Position data of bottom trawling vessels fishing nearby the first mooring location (black dot), (a) during high SSC values from the 31st of October 2011 to the 16th of January 2012, and (b) during low/background SSC values from the 5th to the 18th of October and from the 19th of January to the 20th of February 2012.

et al., 2008). On the other hand, the occurrence of turbidity increases caused by trawling activities over continental slopes has been less investigated. Recent studies conducted on the northwestern Mediterranean slope have described the resuspension effects of bottom trawling over the seafloor, whose effects can be propagated deeper than the fishing grounds (Puig et al., 2012; Martín et al. 2014). These studies were conducted on a submarine canyon flank, where highly-concentrated bottom and intermediate nepheloid layers were generated after the passage of the trawling fleet. Martín et al. (2014) also suggested that trawling activities, by playing an important role in generating near-bottom SSC increases, can currently be the major mechanism involved in the development and maintenance of high-concentration turbid layers on continental slope regions, down to 1000 m depth.

Taking into consideration that the two moorings were located in the middle of currently exploited fishing grounds, and had to be deployed on structural highs to protect the instrumented lines from fishing activities (extending to maximums of 800 m depth), it is very plausible that trawling activity on the GoV continental slope could be the source of the randomly high SSC recorded near the bottom.

To assess the potential role of bottom trawling activities as an active sediment resuspension mechanism, the VMS positions (course and speed) of the trawling vessels operating in the study area were analyzed. VMS data was plotted in two detailed maps nearby the mooring sites, differentiating between periods with high increases of near-bottom suspended sediment concentrations and periods with minimum background turbidity values (Figs. 12 and 13). At the beginning and at the end of the first mooring deployment, from mid-February to end of March 2011, and from mid-April to mid-May 2011, respectively, the suspended sediment concentrations (SSC) records showed values continuously oscillating between 0.6 and 1.6 mg l^{-1}, with several increases up to 3 mg l^{-1} (Fig. 3d). Coinciding with these same two periods, numerous bottom trawling vessels could be tracked nearby and even over the first mooring location (Fig.12a). On the contrary, when minimum or background turbidity values were recorded, from end of March to early April 2011, only few vessels were positioned nearby the mooring site (Fig. 12b).

Similar observations were made for the second mooring site, when during almost the entire deployment, from the end of October 2011 to mid-January 2012, a large number of bottom trawling vessels passed close to and over the mooring site (Fig. 13a). This coincided with repeated increases of suspended sediment concentrations, with values oscillating between 2.5 and 3.5 mg l^{-1} (Fig. 4d). When only background turbidity values were recorded, from beginning to mid-October 2011 and from mid-January to the end of February 2012 (Fig. 4d), just a few bottom trawling vessels were positioned near the mooring site. In addition, most of the vessels were operating down-current from the mooring site (Fig. 13b), and the potential resuspended sediment could not be registered by the moored turbidity sensors since it was mainly advected towards the ESE (Fig. 8c).

Nonetheless, the ultimate dispersion of the resuspended sediment up into the water column and the development of the observed bottom and intermediate nepheloid layers in the GoV (Ribó et al., 2013) seems to be related to the presence of internal waves at depths where the boundary of the LIW and WMDW interacts with the seafloor, as their associated turbulence presumably contributes to maintaining the resuspended particles in the water column and to advecting them seawards.

5. Concluding remarks

The present study describes the hydrographic structure together with the hydrodynamics over the GoV continental slope, improving the understanding on the regional circulation near the bottom and their role in sediment transport.

Intrusions of the Western Mediterranean Intermediate Waters (WIW) were observed during spring 2011 and 2012, largely affecting the near-bottom slope hydrodynamics. In the central part of the GoV continental slope, the WIW intrusion was associated with a change of the current direction that appeared

to be related to the development of a trapped mesoscale anticyclonic eddy. In the southern part of the GoV slope, the intrusion of WIW did not cause major changes on the current direction, but enhanced the unstable behavior of the Northern Current entering into the GoV. Such instabilities were recorded as low-frequency near-bottom current fluctuations, which had a periodicity of 5–20 days, and were attributed to topographic waves.

In general, currents at the study site were mainly south-southeastwards along the slope, with alternating periods of low current velocities (< 10 cm s^{-1}) dominated by near-inertial changes in the current direction, preferentially directed towards the north and offshore. Temperature fluctuations at near-inertial frequencies were also recorded during these low velocity periods, and were associated to the presence of internal waves.

Near-bottom turbidity records show a lack of correlation between increases in SSC and intensification of the current velocity, changes in current direction and oscillations in temperature. Along-slope sediment transport mainly followed the bathymetry of the study site, and was intensified by the current increases driven by the topographic waves. The across-slope dispersion of the suspended sediment is mainly related to the presence of the observed near-inertial internal waves interacting with the seafloor, whose turbulence appears to contribute to the maintenance of the bottom and intermediate nepheloid layers observed over the GoV continental slope.

The sharp and short-lived SSC peaks observed in the records suggest the presence over the GoV of other potential sediment resuspension mechanisms unrelated with current fluctuations. Trawling-induced sediment resuspension is the most plausible mechanism, which seems to play an important role in the present-day GoV sedimentary dynamics.

6. Acknowledgments

This research was supported by the project COSTEM (CTM2009–07806). We thank the captain and the crew of the R/V García del Cid for their assistance. We are grateful to all the UTM technicians and to the Instrumental Service, J. Pozo and M. Lloret, that provided assistance during the data acquisition. M. Ribó is supported by a FPI grant (Ref. BES-2010-029949) from the Spanish Ministry of Economy and Competitiveness.

References

Asper, V.L., Deuser, W.G., Knauer, G.A., Lohrenz, S.E., 1992. Rapid coupling of sinking particle fluxes between surface and deep ocean waters. Nature 357, 670–672.
Bonnin, J., van Haren, H., Hosegood, P., Brummer, G.-J.A., 2006. Burst resuspension of seabed material at the foot of the continental slope in the Rockall Channel. Mar. Geol 226, 167–184. http://dx.doi.org/10.1016/j.margeo.2005.11.006.
Cacchione, D.A., Drake, D.E., 1986. Nepheloid layers and internal waves over continental shelves and slopes. Geo-Mar. Lett 6, 147–152.
Churchill, J.H., 1989. The effect of commercial trawling on sediment resuspension and transport over the Middle Atlantic Bight continental shelf. Cont. Shelf Res. 9, 841–864.
Crépon, M., Wald, L., Monget, J.M., 1982. Low-frequency waves in the Ligurian Sea during December. J. Geophys. Res. 87, 595–600.
Durrieu de Madron, X., Ferré, B., Le Corre, G., Grenz, C., Conan, P., Pujo-Pay, M., Buscail, R., Bodiot, O., 2005. Trawling-induced resuspension and dispersal of muddy sediments and dissolved elements in the Gulf of Lion (NW Mediterranean). Cont. Shelf Res. 25, 2387–2409. http://dx.doi.org/10.1016/j.csr.2005.08.002.
Ferré, B., Durrieu de Madron, X., Estournel, C., Ulses, C., Le Corre, G., 2008. Impact of natural (waves and currents) and anthropogenic (trawl) resuspension on the export of particulate matter to the open ocean. Cont. Shelf Res 28, 2071–2091. http://dx.doi.org/10.1016/j.csr.2008.02.002.
Font, J., 1987. The path of the Levantine Intermediate Water to the Alboran Sea. Deep Sea Res 34, 1745–1755.
Font, J., Salat, J., Tintoré, J., 1988. Permanent features of the circulation in the Catalan Sea. Oceanography, 51–57.
García, E., Tintoré, J., Pinot, J.-M., Font, J., Manriquez, M., 1994. Surface circulation and dynamics of the Balearic Sea. Coast. Estuar. Stud. 46, 73–91.
Guillén, J., Palanques, A., Puig, P., Durrieu de Madron, X., 2000. Field calibration of optical sensors for measuring suspended sediment concentration in the western Mediterranean. Sci. Mar. 64, 427–435.
Hosegood, P., van Haren, H., 2004. Near-bed solibores over the continental slope in the Faeroe-Shetland Channel. Deep Sea Res. Part II 51, 2943–2971. http://dx.doi.org/10.1016/j.dsr2.2004.09.016.
López-Jurado, J.L., Marcos, M., Monserrat, S., 2008. Hydrographic conditions affecting two fishing grounds of Mallorca island (Western Mediterranean): during the IDEA Project (2003–2004). J. Mar. Syst 71, 303–315. http://dx.doi.org/10.1016/j.jmarsys.2007.03.007.
Martín, J., Puig, P., Palanques, A., Ribó, M., 2014. Trawling-induced daily sediment resuspension in the flank of a Mediterranean submarine canyon. Deep Sea Res. Part II 104, 174–183.
McPhee-Shaw, E., 2006. Boundary-interior exchange: reviewing the idea that internal-wave mixing enhances lateral dispersal near continental margins. Deep Sea Res. Part II 53, 42–59. http://dx.doi.org/10.1016/j.dsr2.2005.10.018.
McPhee-Shaw, E., Kunze, E., 2002. Boundary layer intrusions from a sloping bottom: a mechanism for generating intermediate nepheloid layers. J. Geophys. Res. 107, 1–16.
Millot, C., 1999. Circulation in the Western Mediterranean Sea. J. Mar. Syst 20, 423–442. http://dx.doi.org/10.1016/S0924-7963(98)00078-5.
Millot, C., Taupier-Letage, I., 2005. Circulation in the Mediterranean Sea. Handbook of Environmental Chemistry 5, 29–66. http://dx.doi.org/10.1007/b107143 (Part K. pp.).
Monserrat, S., López-Jurado, J.L., Marcos, M., 2008. A mesoscale index to describe the regional circulation around the Balearic Islands. J. Mar. Syst 71, 413–420. http://dx.doi.org/10.1016/j.jmarsys.2006.11.012.
Palanques, A., Puig, P., Guillén, J., 2001. Impact of bottom trawling on water turbitidy and muddy sediment of an unfished continental shelf. Limnol. Oceanogr. 46, 1100–1110.
Palanques, A., Puig, P., Guillén, J., Jiménez, J., Gracia, V., Sánchez-Arcilla, A., Madsen, O., 2002. Near-bottom suspended sediment fluxes on the microtidal low-energy Ebro continental shelf (NW Mediterranean). Cont. Shelf Res. 22, 285–303.
Pinot, J.M., Ganachaud, A., 1999. The role of winter intermediate waters in the spring-summer circulation of the Balearic Sea. Hydrography and inverse box modeling. J. Geophys. Res. 104, 29843–29864.
Pinot, J.-M., López-Jurado, J.L., Riera, M., 2002. The CANALES experiment (1996–1998). Interannual, seasonal, and mesoscale variability of the circulation in the Balearic Channels. Prog. Oceanogr 55, 335–370.
Pinot, J.M., Tintoré, J., Gomis, D., 1994. Quasi-synoptic mesoscale variability in the Balearic Sea. Deep Sea Res. I 41, 897–914.
Pinot, J.M., Tintoré, J., Gomis, D., 1995. Multivariate analysis of the surface circulation in the Balearic Sea. Prog. Oceanogr. 36, 343–376.
Puig, P., Canals, M., Company, J.B., Martín, J., Amblas, D., Lastras, G., Palanques, A., 2012. Ploughing the deep sea floor. Nature 489, 286–289. http://dx.doi.org/10.1038/nature11410.
Puig, P., Palanques, A., Guillén, J., 2001. Near-bottom suspended sediment variability caused by storms and near-inertial internal waves on the Ebro mid continental shelf (NW Mediterranean), Mar. Geol. 178, 81–93.
Puig, P., Palanques, A., Guillén, J., El Khatab, M., 2004. Role of internal waves in the generation of nepheloid layers on the northwestern Alboran slope: implications for continental margin shaping. J. Geophys. Res. 109, 1–11. http://dx.doi.org/10.1029/2004JC002394.
Ribó, M., Puig, P., Salat, J., Palanques, A., 2013. Nepheloid layer distribution in the Gulf of Valencia, northwestern Mediterranean. J. Mar. Syst. 111-112, 130–138. http://dx.doi.org/10.1016/j.jmarsys.2012.10.008.
Robinson, A.R., Leslie, W.G., 2001. Mediterranean Sea Circulation, 1–19. http://dx.doi.org/10.1006/rwos.2001.0376.
Salat, J., 1995. The interaction between the Catalan and Balearic currents in the southern Catalan Sea. Oceanol. Acta 18, 227–234.
Salat, J., Font, J., 1987. Water mass structure near and offshore the Catalan coast during the winters of 1982 and 1983. Ann. Geophys. 5B, 49–54.
Salat, J., Garcia, M.A., Cruzado, A., Palanques, A., Arín, L., Gomis, D., Guillén, J., de León, A., Puigdefàbregas, J., Sospedra, J., R. Velásquez, Z., 2002. Seasonal changes of water mass structure and shelf slope exchanges at the Ebro Shelf (NW Mediterranean). Cont. Shelf Res. 22, 327–348.
Sammari, C., Millot, C., Prieuri, L., 1995. Aspects of the seasonal and mesoscale variabilities of the Northern Current in the western Mediterranean Sea inferred from the PROLIG-2 and PROS-6 experiments. Deep Sea Res. I 42, 893–917.
Schoellhamer, D.H., 1996. Anthropogenic Sediment Resuspension Mechansims in a Shallow Microtidal Estuary. Estuar. Coast. Shelf Sci. 43, 533–548.
Stavrakakis, S., Chronis, G., Tselepides, A., Heussner, S., Monaco, A., Abassi, A., 2000. Downward fluxes of settling particles in the deep Cretan Sea (NE Mediterranean). Prog. Oceanogr. 46, 217–240. http://dx.doi.org/10.1016/S0079-6611(00)00020-3.
van Haren, H., Gostiaux, L., 2011. Large internal waves advection in very weakly stratified deep Mediterranean waters. Geophys. Res. Lett., 38. http://dx.doi.org/10.1029/2011GL049707.
van Haren, H., Laan, M., Buijsman, D.-J., Gostiaux, L., Smit, M.G., Keijzer, E., 2009. NIOZ3: independent temperature sensor sampling yearlong data at a rate of 1 Hz. IEEE J. Ocean. Eng. 34, 315–322.
van Haren, H., Millot, C., 2005. Gyroscopic waves in the Mediterranean Sea. Geophys. Res. Lett. 32, L24614. http://dx.doi.org/10.1029/2005GL023915.
van Haren, H., Ribó, M., Puig, P., 2013. (Sub-)inertial wave boundary turbulence in the Gulf of Valencia. J. Geophys. Res. Ocean 118, 2067–2073. http://dx.doi.org/10.1002/jgrc.20168.
Walsh, J.J., 1991. Importance of continental margins in the marine biogeochemical cycling of carbon and nitrogen. Nature 350, 53–55.